

# Transition from viscous to inertial regime in dense suspensions

Martin Trulsson,<sup>1,\*</sup> Bruno Andreotti,<sup>1</sup> and Philippe Claudin<sup>1</sup>

<sup>1</sup>*Physique et Mécanique des Milieux Hétérogènes,*

*UMR 7636 ESPCI – CNRS – Univ. Paris-Diderot – Univ. P.M. Curie, 10 rue Vauquelin, 75005 Paris, France*

(Dated: July 19, 2022)

Non-brownian suspensions present a transition from a newtonian behaviour in the zero-shear limit to a shear thickening behaviour at large shear rate, none of which is clearly understood so far. Here, we carry out numerical simulations of such an athermal dense suspension under shear, at imposed confining pressure. This set-up is conceptually identical to the recent experiments of Boyer and co-workers [1]. Varying the interstitial fluid viscosities, we recover the Newtonian and Bagnoldian regims and show that they correspond to a dissipation dominated by viscous and contact forces respectively. We show that the two rheological regimes can be unified as a function of a single dimensionless number, by adding the contributions to the dissipation at a given volume fraction.

PACS numbers: 83.80.Hj, 47.57.Gc, 47.57.Qk, 82.70.Kj

The rheology of amorphous materials such as emulsions, foams, metallic glasses, suspensions or granular materials share a similar phenomenology close to the jamming transition at which viscosity diverges [1–4]. However, none of these systems is yet clearly understood and the establishment of a unified theory remains a challenging goal of out of equilibrium statistical physics. Following the pioneering work of Einstein [5], the common view on suspensions of particles in a fluid has long been to start from the dilute limit and to perform an expansion in volume fraction  $\phi$  [6, 7], with a particular emphasis on the effective interaction between particles mediated by the fluid. By contrast, recent studies have started to view the rheology of dense suspensions from the other limit instead, in the framework of dense granular systems [1, 8–11]. The rheology of dense suspensions of solid particles in an iso-dense fluid of viscosity  $\eta_f$  is Newtonian at small shear rate  $\dot{\gamma}$  with a viscosity  $\tau/\dot{\gamma}$  diverging as  $\eta_f(\phi_c - \phi)^{-\beta}$ , as the particle volume fraction goes to its critical value  $\phi_c$ . The measured exponent  $\beta$  ranges between 2 and 3 [1, 12–14]. Mean field theory assuming a dissipation dominated by lubrication films separating particles predicts an exponent  $\beta = 1$  [8]. By contrast, numerical simulations assuming that dissipation is due to the non-affine displacement of particles give the correct exponent  $\beta \simeq 2.2$  [9, 10]. Furthermore, they relate the zero-shear viscosity, a macroscopic dynamical observable, to a microscopic observable: the variance of the non-affine velocity/displacement [9]. The latter is itself related to the geometry of the contact network [10].

While most fluids shear thin, it was first shown by Bagnold [15] that suspensions exhibit shear *thickening* when the volume fraction  $\phi$  is kept constant: their apparent viscosity increases with the shear rate. However, the conditions for such a property to emerge still remain controversial [11]. In particular, as recently emphasized [1], suspensions exhibit shear *thinning* when the confining pressure  $P^p$  is controlled and kept constant, a property reminiscent of dry granular materials.

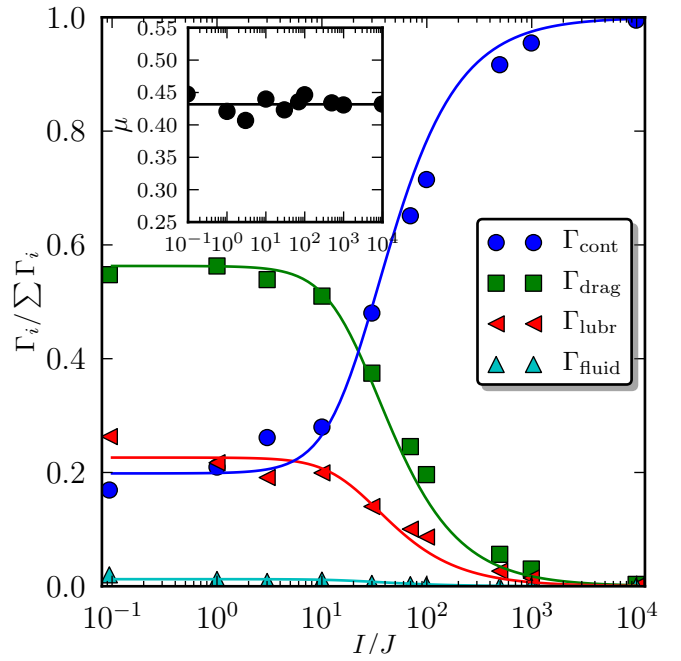


FIG. 1: Fraction of the power dissipated by contact forces ( $\Gamma_{\text{cont}}$ ), viscous drag ( $\Gamma_{\text{drag}}$ ), lubrication forces ( $\Gamma_{\text{lubr}}$ ) and fluid viscosity ( $\Gamma_{\text{fluid}}$ ), as a function of the ratio  $I/J$  for a fixed value of the volume fraction ( $\phi \simeq 0.78$ ). Solid lines are the best fits to the expression  $\frac{c_i J}{J + \alpha I^2}$ , with  $c_i$  as fitting parameters, for the three last dissipation components. Inset: Friction coefficient  $\mu$  against  $I/J$ . Solid curve illustrates the average  $\mu$ .

In this letter, we use discrete element simulations of non-brownian particles interacting with a continuum viscous fluid to show that the rheology of suspensions at finite shear rate can be unified with the Newtonian quasi-static limit. More precisely, Boyer *et al.* [1] have recently shown that the rheology of a suspension in the zero-shear limit can be rewritten as a frictional law of the form

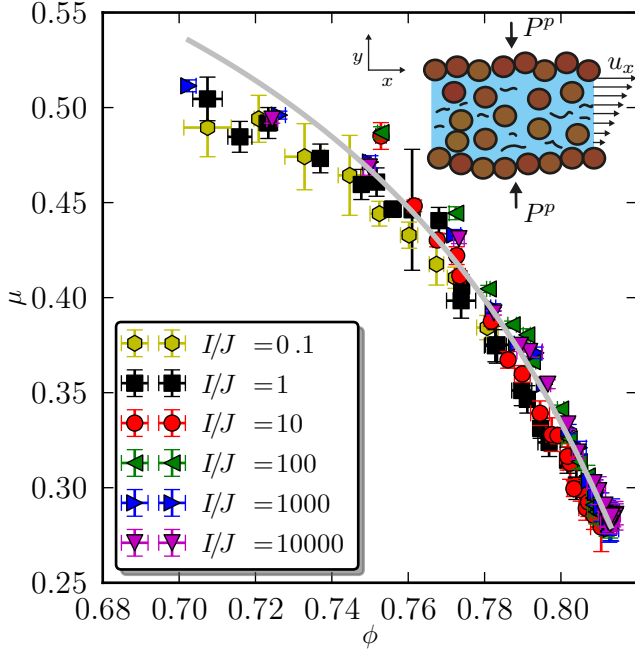


FIG. 2: Friction coefficient of the suspension  $\mu = \tau/P^p$  as a function of the particle volume fraction  $\phi$ , for different values of  $I/J$ . The solid line is the best fit by Eq. 8. Inset: numerical set-up and notations.

$\tau = \mu_J(J)P^p$  and  $\phi = \phi_J(J)$ , where  $J = \eta_f \dot{\gamma}/P^p$  is the viscous number comparing viscous stresses to the confining pressure. In the inertial Bagnoldian regime, the flow is characterized by the inertial number  $I = \sqrt{\rho \dot{\gamma}^2 d^2 / P^p}$ , with a subsequent rheology of the form  $\tau = \mu_I(I)P^p$  and  $\phi = \phi_I(I)$ . We show here that the contributions to the dissipation can be added at fixed  $\phi$ , which results into a unique rheology  $\tau = \mu(K)$  and  $\phi(K)$  controlled by the dimensionless number  $K = J + \alpha I^2$ , where  $\alpha$  is a constant of order 1 encoding the details of dissipative mechanisms.

*Numerical model* – We consider a two-dimensional system constituted of  $\simeq 10^3$  spherical particles of mass  $m_i$  and diameter  $d_i$ , with a  $\pm 50\%$  polydispersity. The shear cell is composed by two rough walls, created by gluing together two dense layers of grains, with periodic boundary conditions along the direction  $x$  parallel to the walls. The position of the walls is controlled to insure a constant normal stress  $P^p$  and a constant mean shear velocity  $\dot{\gamma}$ . The particle and wall dynamics are integrated using a Verlet-algorithm. These discrete elements are coupled to a density matched fluid, described as a slowly varying continuum phase. In the steady state, the fluid presents only variations along the transverse axis  $y$ . The velocity  $\mathbf{u}^f(y)$  and the shear stress  $\boldsymbol{\sigma}^f(y)$  profiles are determined by averaging the equations governing the motion of the fluid over  $x$  and over time  $t$ , as proposed in [16].

The particles are submitted to four types of forces. (i) Upon contact, they interact with a viscoelastic force and with a Coulomb friction for relative tangential motion between particles at contact [17–19]. The model used for particle-particle interactions is identical to that proposed by Luding [19], with  $k_n = 10^4$  (normal spring constant),  $k_t = 0.5k_n$  (tangential spring constant),  $\beta_n = 6.70$  (normal damping),  $\beta_t = 4.74$  (tangential damping), and  $\mu_p = 0.4$  (coulomb friction). This corresponds to a restitution coefficient  $e \simeq 0.9$ . (ii) They are submitted to a viscous drag force given by:

$$\mathbf{f}_i^{\text{drag}} = 3\pi\eta_f d_i (\mathbf{u}^f(y_i) - \mathbf{u}_i^p) \quad (1)$$

which involves the non-affine particle velocity component, *i.e.* the fluid velocity  $\mathbf{u}^f$  minus the particle velocity  $\mathbf{u}^p$ . This is based on the assumption that the particle based Reynolds numbers  $\text{Re}_p = \frac{\rho |\mathbf{u}^p - \mathbf{u}^f| d}{\eta_f}$  remains small. (iii) When the fluid presents a stress gradient, it exerts a resultant Archimedes force on the particle, which reads  $\mathbf{f}_i^{\text{archi}} = (\pi d_i^2 / 4) \nabla \cdot \boldsymbol{\sigma}^f$ . (iv) Finally, when particles are separated by a lubrication film, we include the extra-stress as an interparticle force mediated by the fluid [21]:

$$\mathbf{f}_{ij}^{\text{lubr,n}}(h_{ij}) = -\frac{3}{4}\pi\eta_f d_{ij} \frac{(\mathbf{u}_i^p - \mathbf{u}_j^p) \cdot \mathbf{n}_{ij}}{(h_{ij} + \delta)} \quad (2)$$

$$\mathbf{f}_{ij}^{\text{lubr,t}}(h_{ij}) = -\pi\eta_f \ln\left(\frac{d_{ij}}{2(h_{ij} + \delta)}\right) (\mathbf{u}_i^p - \mathbf{u}_j^p) \cdot \mathbf{t}_{ij} \quad (3)$$

where  $h_{ij}$  is the gap between the particles labelled  $i$  and  $j$ ,  $d_{ij} = \frac{2d_i d_j}{d_i + d_j}$  is the effective grain diameter,  $\mathbf{n}_{ij}$  and  $\mathbf{t}_{ij}$  are the normal and tangential unit vectors between the grains.  $\delta$  is a regularisation length, chosen equal to 10% of particle diameter. In real suspensions, it can be either related to the slip length, to the grain roughness or to the scale over which grains are elastically deformed [20]. This lubrication interaction is cut for  $h_{ij} > (d_i + d_j)/4$ .

As the fluid is described as a continuum phase in a steady state, inertial effects and non-affine effects are entirely ascribed to the particle phase. This means that the density  $\rho$  only appears in the equation of motion for the grains and include the added-mass effect.

As obtained for dense granular flows [17], the simulation is insensitive to microscopic parameters provided that the grains are hard enough. The state of the system is then characterised by the two dimensionless numbers  $I$  and  $J$ . In the following, we will rather use the Stokes number  $I^2/J = \rho \dot{\gamma}^2 d^2 / \eta_f$  and the rescaled confining pressure  $I/J = \sqrt{\rho P^p d} / \eta_f$ .

*Transition from viscous to inertial regime* – Figure 1 presents simulation results obtained at the same volume fraction  $\phi \simeq 0.78$  by varying the rescaled confining pressure  $I/J$ . It compares the contributions to the dissipated power of the different forces acting on the bulk of the suspension. This dissipation is balanced by the energy

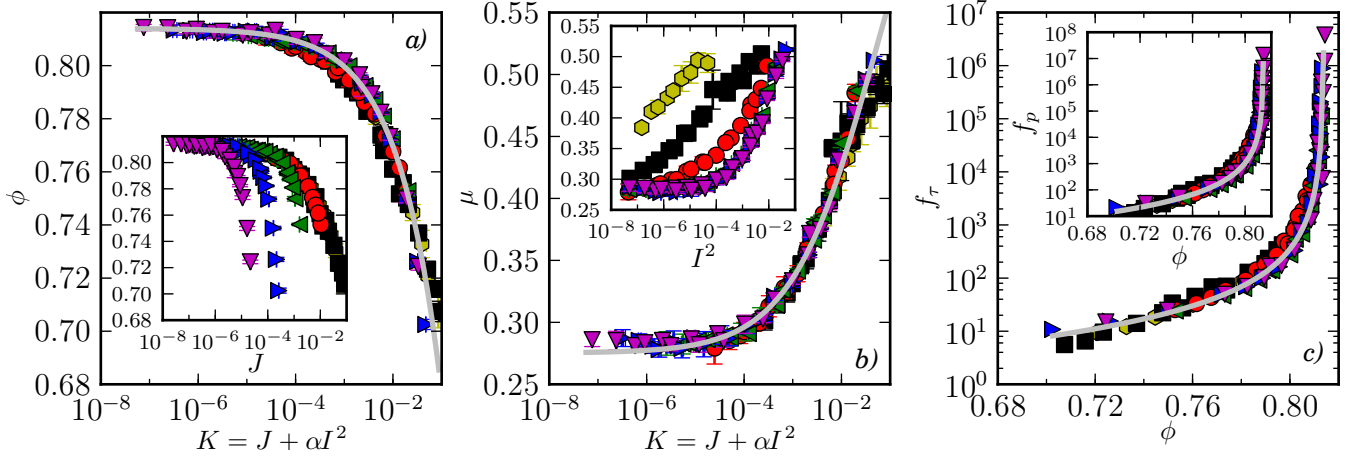


FIG. 3: Simulated data. *a*):  $\phi$  as a function of  $K$  (inset as a function of  $J$ ). *b*):  $\mu$  as a function of  $K$  (inset as a function of  $I^2$ ). *c*):  $f_\tau$  as a function of  $\phi$  (inset shows  $f_p$ ). All three figures are for various  $I/J$  with the same color coding as in Figure 2. Solid lines corresponds to fits accordingly to Eqs. 6,7,  $f_\tau = \mu/K$  and  $f_p = 1/K$ .

bought through the boundary of the element of suspension considered. While the dissipation due to the drag force is dominant at small  $I/J$ , the dissipation in the contacts becomes dominant at large  $I/J$  and the system resembles a dry granular flow (within the inclusion of the added mass effect inside the density  $\rho$ ). The system therefore presents a transition from a viscous to an inertial regime, controlled by the rescaled pressure. It can be seen that the dissipation in the fluid, both in the pores and in the lubrication films, gives a subdominant contribution and vary like the contribution due to the drag force. In the following, we will therefore focus on results obtained without the lubrication forces.

Looking at the inset of Figure 1, one observes that the friction coefficient  $\mu$  defined as the ratio of the particle shear stress  $\tau^p$  and confining pressure  $P^p$  remains constant across the transition. This means that, at fixed  $\phi$ , the shear stress is controlled by pressure, with a multiplicative factor insensitive to the nature of the dissipation mechanisms. Figure 2 shows the friction coefficient  $\mu$  of the system as a function of the volume fraction  $\phi$  for different values of the number  $I/J$ . A good data collapse is obtained, when  $I/J$  is changed over five decades, showing that  $\mu$  is sole function of  $\phi$ . This suggests the existence of a hidden universality underlying the transition between regimes.

*A single rheology across the transition* – It has been recently argued that trajectories are mostly controlled by geometric effects close to the jamming point, and do not depend much on the nature of the mechanisms dissipating energy [9]. This suggests that grain trajectories do not vary much across the viscous/turbulent transition. We therefore hypothesise that, for a given volume fraction  $\phi$ , the dissipation due to viscous effects and that due to grain binary interactions can simply be added. Then,

particle shear stress and confining pressure can be written as sums of linear (viscous) and quadratic (Bagnold) terms in  $\dot{\gamma}$  [1, 8, 22, 23]:

$$\tau^p = f_\tau(\phi) (\eta_f \dot{\gamma} + \alpha \rho d^2 \dot{\gamma}^2), \quad (4)$$

$$p^p = f_p(\phi) (\eta_f \dot{\gamma} + \alpha \rho d^2 \dot{\gamma}^2), \quad (5)$$

Although the parameter  $\alpha$  *a priori* depends on  $\phi$ , the best fit of  $\mu$  and  $\phi$ , functions of  $I$  and  $J$ , rather give a constant value  $\alpha = 0.458 \pm 0.007$  (Fig. 3a,b). Indeed, we obtain a collapse of all data when  $\mu$  and  $\phi$  are plotted against  $K = J + \alpha I^2$ . Consistently, expressions (4) and (5) give the two relations:  $\phi = f_p^{-1}(1/K)$  and  $\mu = f_\tau(\phi)/f_p(\phi)$ . Following empirical expressions proposed for  $\phi$  and  $\mu$  as functions of  $I$  or  $J$  in the cases of dry granular flows and dense suspension respectively [1, 17, 22], we can generalize them using the number  $K$  as

$$\phi(K) = \phi_c - b\sqrt{K}, \quad (6)$$

$$\mu(K) = \mu_c + \frac{\mu_F - \mu_c}{1 + \sqrt{K_0/K}}. \quad (7)$$

where  $\phi_c = 0.8140 \pm 0.0003$  is the jamming volume fraction. The constants  $b$ ,  $\mu_c$ ,  $\mu_F$ , and  $K_0$  are specific to the considered system. Here we find,  $b = 0.42 \pm 0.01$ ,  $\mu_c = 0.275 \pm 0.001$ ,  $\mu_F = 0.49 \pm 0.01$  and  $K_0 = 0.223 \pm 0.008$ . Combining the two constitutive laws we finally get

$$\mu(\phi) = \mu_c + \frac{\mu_F - \mu_c}{1 + \sqrt{K_0 b / (\phi_c - \phi)}}. \quad (8)$$

This expression is in good agreement with the data displayed in figure 2. Furthermore, as  $f_\tau = \mu/K$  and  $f_p = 1/K$ , these two functions are predicted to diverge close to the jamming point as  $(\phi_c - \phi)^{-2}$ , as a consequence of Eq. 6. This behavior is also very well supported by our data, as seen in Figure 3c.

We have run simulations in which lubrication interactions between the grains are taken into account. They do not affect the qualitative results described above but slightly change the values of the constants. In particular, the exponent of the diverging behavior of both functions  $f_\tau$  and  $f_p$  is unchanged. This contradicts the claim of [8] that the divergence would be in  $(\phi_c - \phi)^{-1}$  when lubrication forces are present.

*Discussion* – The above analysis shows a cross-over from viscous to inertial flow at a Stokes number  $I^2/J = \dot{\gamma}d^2\rho_s/\eta_f \simeq 1/\alpha$ . The suspension is therefore found to shear-thicken when  $I^2/J$  is comparable to or above this value. In the experiments of Boyer *et al.*, the maximum value of the Stokes number can be estimated as  $10^{-3}$ . This value is far below the inertial regime, and, consistently, all their rheological data collapse when using  $J$  as the single dimensionless parameter [1]. By contrast, Fall *et al.* report in their experiments a cross-over between the two regimes, at a Stokes number of  $2 \cdot 10^{-3}$  [11]. This value is three to four orders of magnitude lower than the predictions of our simulations. We hypothesise that this effect may result from non-local effects, as the base flow is heterogenous. The dominant influence of non-locality has previously been observed before in other heterogenous flows of dense suspensions [24], emulsions [25], and granular systems [26–28]. Our set-up is insensitive to non-local effects as all studied quantities are homogeneous over the shear-cell. Nevertheless, many flows are heterogenous and it would be important to understand non-locality in order to rationalize even these.

Newtonian fluids exhibit a transition from laminar to turbulent flow controlled by the Reynolds number based on the size of the flow and on the suspension viscosity. It is unlikely that dilute or even moderately concentrated suspensions would be an exception to this rule. As the jamming transition is approached ( $\phi \rightarrow \phi_c$ ), the suspension viscosity diverges so that the Reynolds number vanishes. The transition from the viscous to the inertial regime in dense suspension is thereby of a different nature than the transition from laminar to turbulent flow. In the former, both the Newtonian and Bagnoldian regimes are controlled by particle fluctuations with respect to the affine field. These fluctuations are controlled by the Stokes number, which is based on the grain diameter and the fluid viscosity rather than the suspension viscosity. Further studies are needed to investigate the transition from the inertial regime to the turbulent regime when the particle volume fraction is lowered.

In this letter, we have shown that the Newtonian rheology of suspensions can be unified with the Bagnoldian shear-thickening regime for vanishing temperature. As pointed out recently by Ikeda *et al.* [29], thermal and athermal suspensions seem physically distinct, making an unified description of glass and jamming transitions unlikely. Future studies will have to explain the difference in nature (if any) between mechanically induced fluctua-

tions (*i.e.* non-affine motion) at zero temperature and thermal fluctuations.

We thank Orencio Durán for support with the DEM code. We thank E. Clément, J. Kurchan and A. Lindner for discussions. This work is funded by ANR JamVibe.

---

\* Electronic address: martin.trulsson@espci.fr

- [1] F. Boyer, E. Guazzelli, and O. Pouliquen, Phys. Rev. Lett. **107**, 188301 (2011)
- [2] B.P. Tighe, E. Woldhuis, J.J.C. Remmers, W. van Saarloos, and M. van Hecke, Phys Rev Lett **105**, 088303 (2010)
- [3] D.J. Durian, Phys. Rev. Lett. **75**, 4780 (1995)
- [4] P. Olsson and S. Teitel, Phys Rev Lett **99**, 178001 (2007)
- [5] A. Einstein, Ann. Phys. (Berlin) **322**, 549 (1905)
- [6] E. Guazzelli and J. F. Morris, *A Physical Introduction to Suspension Dynamics* (Cambridge University Press, Cambridge, 2012)
- [7] G. Batchelor, J. Fluid Mech. **83**, 97 (1977)
- [8] P. Mills and P. Snabre, Eur. Phys. J. E **30**, 309 (2009)
- [9] B. Andreotti, J.-L. Barrat, and C. Heussinger, [arXiv:1112.1194v1](#) [cond-mat.soft] (2011)
- [10] E. Lerner, G. Düring, and M. Wyart, [arXiv:1112.0558v3](#) [cond-mat.soft] (2012)
- [11] A. Fall, A. Lemaitre, F. Bertrand, D. Bonn, and G. Ovarlez, Phys. Rev. Lett. **105**, 268303 (2010)
- [12] I. E. Zarraga, D. A. Hill, and D.T. Leighton, J. Rheology **45**, 1065 (2001)
- [13] G. Ovarlez, F. Bertrand, and S. Rodts, J. Rheol. **50**, 259 (2006)
- [14] C. Bonnoit, T. Darnige, E. Clément, and A. Lindner, J. Rheol. **54**, 65 (2010)
- [15] R. A. Bagnold, Proc. R. Soc. Lond. A **225**:(1160), 49 (1954)
- [16] O. Durán, B. Andreotti and P. Claudin Submitted to Phys. Fluids, [arXiv:1111.6898](#).
- [17] F. da Cruz, S. Emam, M. Prochnow, J. N. Roux, and F. Chevoir, Phys. Rev. E **72**, 021309 (2005)
- [18] P. A. Cundall, O. D. L. Strack, Geotechnique **29**, 4765 (1979)
- [19] S. Luding, Behavior of Granular Media, p137–147 (2006)
- [20] P.G. Rognon, I. Einav, C. Gay, J. Fluid Mech. **689**, 75 (2011)
- [21] R.G. Cox, Int. J. Multiphase Flows **1**, 343 (1974)
- [22] GDR MiDI, Eur. Phys. J. E **14**, 341 (2004)
- [23] C. Cassar, M. Nicolas, and O. Pouliquen, Phys. Fluids **17**, 103301 (2005)
- [24] C. Bonnoit, J. Lanuza, A. Lindner and E. Clément, Phys. Rev. Lett. **105**, 108302 (2010)
- [25] J. Goyon, A. Colin, G. Ovarlez, A. Ajdari, and L. Bocquet, Nature **454**, 84 (2008)
- [26] B. Andreotti, Europhys. Lett. **79**, 34001 (2007).
- [27] O. Pouliquen and Y. Forterre, Phil. Trans. R. Soc. A **367**, 5091 (2009)
- [28] K. A. Reddy, Y. Forterre, and O. Pouliquen, Phys. Rev. Lett. **106**, 108301 (2011)
- [29] A. Ikeda, L. Berthier, and P. Sollich, [arXiv:1203.0825](#) [cond-mat.soft] (2012)